Advances in Aircraft and Spacecraft Science, *Vol. 5, No. 4 (2018) 411-430*
DOI: https://doi.org/10.12989/aas.2018.5.4.411

Influence of fin partitioning of a Rayeigh-Bénard cavity at low Rayleigh numbers

Adis Zilic[a] and Darren L. Hitt[*]

Department of Mechanical Engineering, University of Vermont, Burlington, Vermont, USA

(Received July 22, 2017, Revised November 29, 2017, Accepted January 15, 2018)

Abstract. This computational study examines the augmentation of classic 2-D Rayleigh-Bénard convection by the addition of periodically-spaced transverse fins. The fins are attached to the heated base of the cavity and serve to partition the cavity into 'units' with different aspect ratios. The respective impacts upon heat transfer of the fin configuration parameters – including spacing, height, thickness and thermal conductivity – are systematically examined through numerical simulations for a range of laminar Rayleigh numbers ($0 < Ra < 2 \times 10^5$) and reported in terms of an average Nusselt number. The selection of the low Rayleigh number regime is linked to likely scenarios within aerospace applications (e.g. avionics cooling) where the cavity length scale and/or gravitational acceleration is small. The net heat transfer augmentation is found to result from a combination of competing fin effects, most of which are hydrodynamic in nature. Heat transfer enhancement of up to 1.2× that for a Rayleigh-Bénard cavity without fins was found to occur under favorable fin configurations. Such configurations are generally characterized by short, thin fins with half-spacings somewhat less than the convection cell diameter from classic Rayleigh-Bénard theory. In contrast, for unfavorable configurations, it is found that the introduction of fins can result in a significant reduction in the heat transfer performance.

Keywords: natural convection; Rayleigh-Bénard cells; low Rayleigh number; passive cooling; heat transfer with partitions

1. Introduction

Natural convection is regarded as an attractive mode of cooling when simplicity, economy, reliability and noise become constraint parameters of importance. In view of this, natural convection has been the subject of considerable interest in the cooling of heat exchange devices in industry (e.g., electric transformers, HVAC equipment, electronic components). An important subclass of problems on natural convection deals with confined flows that are induced inside enclosures when a temperature differential is prescribed at two or more walls; several state-of-the-art reviews devoted to natural convection in enclosures have been published in the past by various authors (Ostrach 1972, Catton 1978, Hoogendoorn 1986, Hollands *et al*. 1976, Jaluria 2003).

Over the years, theoretical analyses, numerical simulations and experimental measurements have been directed to the issue of heat transfer intensification. State-of-the-art review articles on

*Corresponding author, Professor, E-mail: dhitt@uvm.edu
[a]M.Sc. Student, E-mail: azilic@gmail.com

Copyright © 2018 Techno-Press, Ltd.
http://www.techno-press.org/?journal=aas&subpage=7 ISSN: 2287-528X (Print), 2287-5271 (Online)

this important topic have regularly appeared in the literature. A variety of enhancing schemes for forced convection in tube flows have been investigated throughout the years and a detailed survey of them may be found in the heat transfer literature (e.g. Bergles (1999), Manglik (2003)). This valuable information provides guidance to engineers that are engaged in the design of tubes for high-performance heat exchange devices. In general, enhancement schemes have been classified into two broad categories: (a) passive methods requiring no application of external power or (b) active methods that demand the use of external power. One passive method that is commonly used in industry deals with the intentional extension of the internal surface areas of tube walls by roughening, corrugating or finning. The increase of the internal surface areas amplifies the heat transfer rates, but also increases the friction factor and the pressure drop. As an undesirable consequence, the power requirement for the pump to sustain the fluid flow is also increased. Thus, it is of fundamental and practical interest to explore passive instruments that are conducive to heat transfer augmentation that are power-independent; this is particularly true of space-based applications where energy consumption must be minimized.

When natural convection occurs in confined spaces, such as enclosures or partitioned regions, the fluid physics dictate that the enhancement of heat transport becomes difficult because of the low fluid velocities associated with buoyancy-driven flows. In this article we examine the augmentation of classic Rayleigh-Bénard convection by the addition of periodically-spaced tranverse fins (or 'ribs') attached to the heated, lower boundary. While the literature on natural convection in enclosures is itself vast, the information dealing with this particular thermal design strategy is less so (Lin and Bejan 1983, Arquis and Rady 2005, Amraqui *et al*. 2011, El Qarnia *et al*. 2013, Ahmadi *et al*. 2014, Sivaprakasam *et al*. 2015, Singh and Sinha 2016, Beldar and Patil 2017). The primary sources of experimental data are found to be the studies by Inada *et al*. (1999) and, to a lesser degree, the more recent work of Sivaprakasam *et al*. (2015). The study by Inada, Taguchi and Yang (1999) indicated that the inclusion of transverse fins had the overall effect of enhancing the natural convective flows and that the enhancement scaled with the Rayleigh number. The experiments were restricted to a limited number of parametric conditions (i.e., three fin spacings, a single fin size) and thus the data reported was somewhat limited in scope. We have taken the experimental results of Inada *et al*. (1999), along with the earlier numerical simulations of Arquis and Rady (2005) as motivation to extend this important, fundamental work and to expand the number and scope of parametric conditions through the use of computational fluid dynamics (CFD) simulations.

The present investigation is focused on a low Rayleigh number regime with associated laminar flows. This selection corresponds to likely scenarios encountered in aerospace applications, such as passive avionics cooling. For aircraft avionics, the compact size of the avionics packaging leads to air enclosures with small aspect ratios (i.e., height-to-width). As the Rayleigh number scales with the cube of the air gap, the Rayleigh number will necessarily be small. Spacecraft avionics cooling affords another important application. Although there is no formal gravitational acceleration in space, satellites in orbit can be subject to so-called 'g-jitter'; this term refers to accelerations produced in orbit by various aerodynamic/aeromechanical forces, equipment operation and/or crew activity (Nelson 1994). The g-jitter effects, consequently, have been the subject of various studies on transport processes in space (e.g., Naumann (2000), Kanashima *et al*. (2005)). Another source of low-level acceleration in spacecraft arises in modern electric propulsion systems (EP). In contrast to the high-thrust, impulsive behavior of chemical propulsion systems, EP systems are characterized by low-level continuous thrust and acceleration. For example, NASA's DAWN Mission to the asteroids Ceres and Vesta featured an ion engine generating a

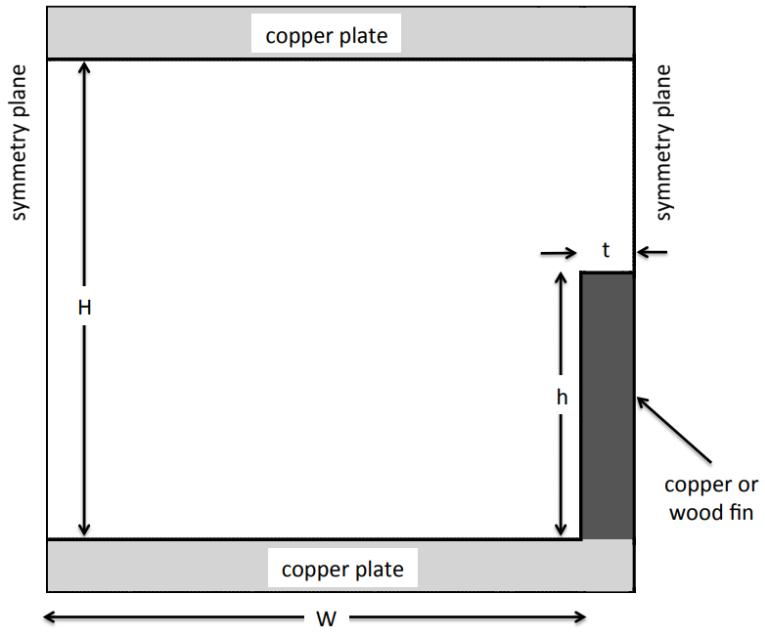

Fig. 1 Schematic diagram illustrating the geometry of the computational domain. The transverse fins in a particular simulation can be either copper (conducting) or wood (insulating)

maximum acceleration of 0.4 m/s^2 for this 1200 kg probe (Rayman *et al*. 2006). In such cases, the constant low-level acceleration will likely establish near steady-state natural convection within the spacecraft avionics.

The outcomes of this study provide a detailed, systematic and comprehensive understanding of the heat transport augmentation introduced in natural convection enclosures through the addition of transverse fins. Extensive parametric studies serve to identify fin configurations that offer enhancement of heat transport relative to the standard Rayleigh-Bénard scenario, as well as those that prove detrimental to performance. In turn, the findings of this work may prove useful for both fundamental research and thermal design and specifically within the aforementioned aerospace avionic cooling scenarios.

2. Numerical methods

A two-dimensional computational model has been created in order to numerically study the augmentation of the convective heat transfer in a classic Rayleigh-Bénard configuration arising from the addition of a periodic array of transverse fins. For the present study, we have restricted our investigation to the case of laminar flows. The computational approach taken here is a modified version of the one previously described by Papari *et al*. (2005). A schematic diagram of the geometry of the computational domain for this study appears in Fig. 1, which represents a single 'unit cell' from which an infinite, periodic domain could be constructed. Accordingly, the left and right domain boundaries are taken as symmetry planes. The unit cell is bounded above and below by two rigid, thermally-conducting plates of width W separated by a uniform gap H; the

actual fin spacing is thus $2W$. For this study, we assume the bounding plate material to be copper; this material choice reflects typical experimental methods used in imposing isothermal boundary conditions. Attached to the bottom plate is a thin vertical fin defined to be of width t and a height h. The fin material may be either thermally-conducting (copper) or non-conducting (wood). As the ratio W/H becomes sufficiently large, the impact of a fin diminishes and one expects a trend approaching the idealized case of Rayleigh-Bénard convection between infinite parallel plates. With this in mind and consistent with the experiments of Inada *et al*. (1999), emphasis in this study is placed on 'close' fin spacings – that is, fin spacings less than or equal to the diameter of a 2-D roll pattern in the idealized Rayleigh-Bénard case. For the numerical studies, we assume a fixed gap width of H = 9 mm and a fin half-width of t =1 mm unless otherwise stated. Fin heights considered include h =1mm, 5 mm and 8 mm. The corresponding fin aspect ratios are h/H =0.11, 0.55 and 0.88 and are intended to represent cases of 'short', 'intermediate' and 'tall' fins.

Owing to the simplicity of the domain, the computational mesh consists completely of quadrilateral elements with zero-skewness. A uniform grid resolution of 0.05 mm is used for the horizontal and vertical directions and has been found to yield solutions which are insensitive to further refinement. The exact number of computational cells scales linearly with fin spacing; as an illustration, a simulation with W/H=1.2 mm has a mesh consisting of approximately 23,000 cells.

The governing equations for the natural convection flow are the steady, compressible 2-D Navier-Stokes (Boussinesq) equations along with the energy equation and the equation of state:

$$\nabla \cdot (\rho \boldsymbol{u}) = 0 \tag{1}$$

$$\nabla \cdot (\rho \boldsymbol{uu}) = -\nabla p + \rho \boldsymbol{g} + \mu \nabla^2 \boldsymbol{u} \tag{2}$$

$$\nabla \cdot \left[\rho \boldsymbol{u}\left(C_p T + \frac{1}{2}|\boldsymbol{u}|^2\right)\right] = \nabla \cdot [k \nabla T] \tag{3}$$

$$p = \rho R T \tag{4}$$

$$\rho = \rho_0[1 - \beta(T - T_0)] \tag{5}$$

Air has been used as the working fluid in all simulations. The Boussinesq approximation has been utilized for the modeling of the body force and is referenced to the mean temperature T_0 between the hot and cold plates. In all numerical studies performed, constant temperatures of T_h=310 K and T_c=290 K have been imposed on the lower and upper plates, respectively. For air, at this mean temperature and a modest temperature differential of 20K, the Boussinesq approximation is well justified. The thermophysical properties of air over this temperature range exhibit only a minor variation and therefore have been assumed constant in the simulations. Specifically, the property values used are evaluated at the mean temperature $T_0 = (T_h + T_c)/2 = 300$ K. Perfect gas behavior is assumed. As such, the enthalpy is given by C_pT and the thermal expansion coefficient for the perfect gas is given by $\beta = -\rho^{-1} (\partial\rho/\partial T)_p = T_0^{-1}$. For completeness, the energy equation here retains the kinetic energy term although it is essentially negligible for the natural convection flow.

The system of equations (1) - (5) is solved using a CFD code based on the finite volume method. An implicit segregated solver is used and all discretization schemes employed are of second-order accuracy or higher. A quadratic upwinding scheme (QUICK algorithm) is used for the momentum, energy and density discretization. A second-order body-force-weighted scheme is

Table 1 Correlation of gravity values and Rayleigh numbers in the numerical simulations

Gravitational Constant (g's)	Rayleigh Number
1	1.971×10^3
5	9.856×10^3
10	1.971×10^4
20	3.942×10^4
30	5.914×10^4
40	7.885×10^4
50	9.856×10^4
60	1.183×10^5
70	1.380×10^5
80	1.577×10^5
90	1.774×10^5
100	1.971×10^5

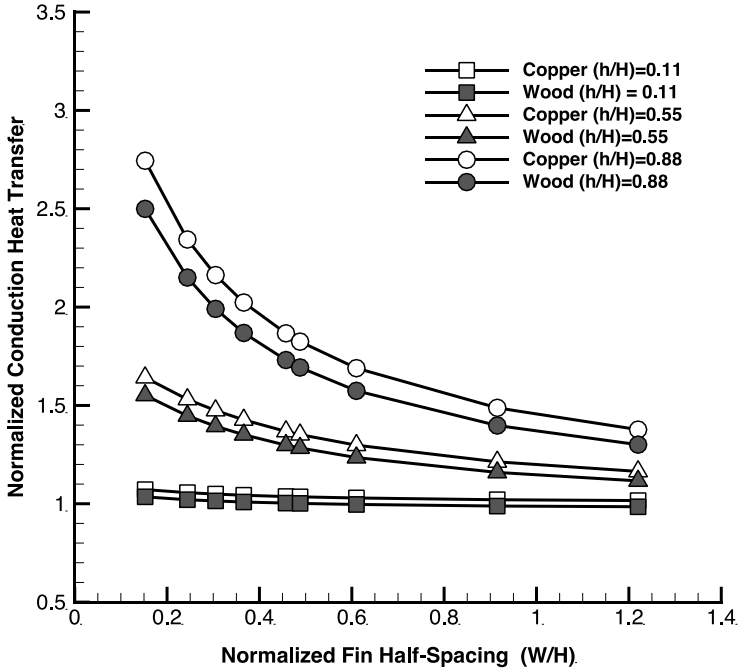

Fig. 2 Normalized conduction heat transfer rates for different fin heights, spacing and materials relative to a that for a parallel plate configuration. Only spacings up to W/H =1.2 are shown

used in the pressure discretization and the SIMPLE scheme is used in the pressure-velocity coupling. Convergence of a simulation is assessed through the monitoring of computed residuals (velocity, energy and mass conservation) and also through the convergence of point and/or surface monitors for velocity, temperature and heat flux at selected locations in the domain. For a simulation starting from an initially quiescent conduction profile, approximately 40,000 iterations are required for complete convergence. Once a solution is obtained, the local heat flux distribution is computed on the lower (or upper) plate and then integrated over the entire surface to obtain the total heat transfer Q (per unit depth).

The appropriate definition of the Nusselt number for this problem is

$$Nu = \frac{Q}{Q_{cond}} \tag{6}$$

where Q_{cond} is the heat transfer associated with a purely conductive state. Note the conduction heat transfer must be a computed quantity since the presence of a fin alters the base conduction state for a particular geometry. For natural convective flows, it is expected that the Nusselt number will scale as a function of the Rayleigh number,

$$Ra = \frac{\rho g \beta (T_h - T_c) H^3}{\nu \alpha} \tag{7}$$

where ρ is the density, g is the gravitational constant and ν, α are the viscous and thermal diffusivities, respectively. For a given geometry, mean operating temperature and thermophysical properties of air, a range of Rayleigh numbers can be realized through the (artificial) variation of the gravitational constant g. In this study, we restrict the range of Rayleigh numbers so as to ensure a laminar flow condition exists; the relation between artificial gravitational values and the corresponding Rayleigh number appears in Table 1. The reference and baseline for assessing heat transfer augmentation due to fins is the classic 2-D Rayleigh-Bénard convection flow between infinite parallel plates. Numerical values are obtained using the empirical correlation reported by Hollands *et al*. (1976):

$$Nu = 1 + 1.44 \left\| 1 - \frac{1708}{Ra} \right\| + \left\| \left(\frac{Ra}{5830} \right)^{1/3} - 1 \right\| \tag{8}$$

In this formula, the notation $\|\cdot\|$ indicates that the bracketed term is taken to be zero if its argument is negative. This correlation equation has been shown to yield excellent agreement with experiments over the entire laminar flow regime.

3. Results

In the following sections, we report on the calculated Nusselt numbers obtained from numerical simulations under a range of parametric conditions. Specifically, the respective impacts of Rayleigh number, fin spacings and heights and fin thermal conductivities are delineated. As a necessary first step, the heat transfer rates have been computed for different fin configurations and materials under a state of pure conduction. Knowledge of these baseline heat transfer values are required for the expression of the natural convective heat transfer rates in terms of a Nusselt number according to Eq. (6). Normalized results appear in Fig. 2 for three different non-dimensional fin heights considered. To highlight the conductive heat transfer enhancement of the fin, these results are presented as a 'fin effectiveness' with the values normalized by the 1-D conduction rate that would exist between parallel plates without a fin, i.e.,

$$Q_{nofin} = kQ \left[\frac{T_h - T_c}{H} \right] \tag{9}$$

As might be expected, the fin extension into the air gap enhances the conduction heat transfer in all cases. The enhancement scales with the fin height and is somewhat greater for a conductive fin than an insulating fin. For the smallest fins, there is little enhancement overall and only minor effects of the fin material. The greatest fin impact is felt for the closest fin spacing. As the fin

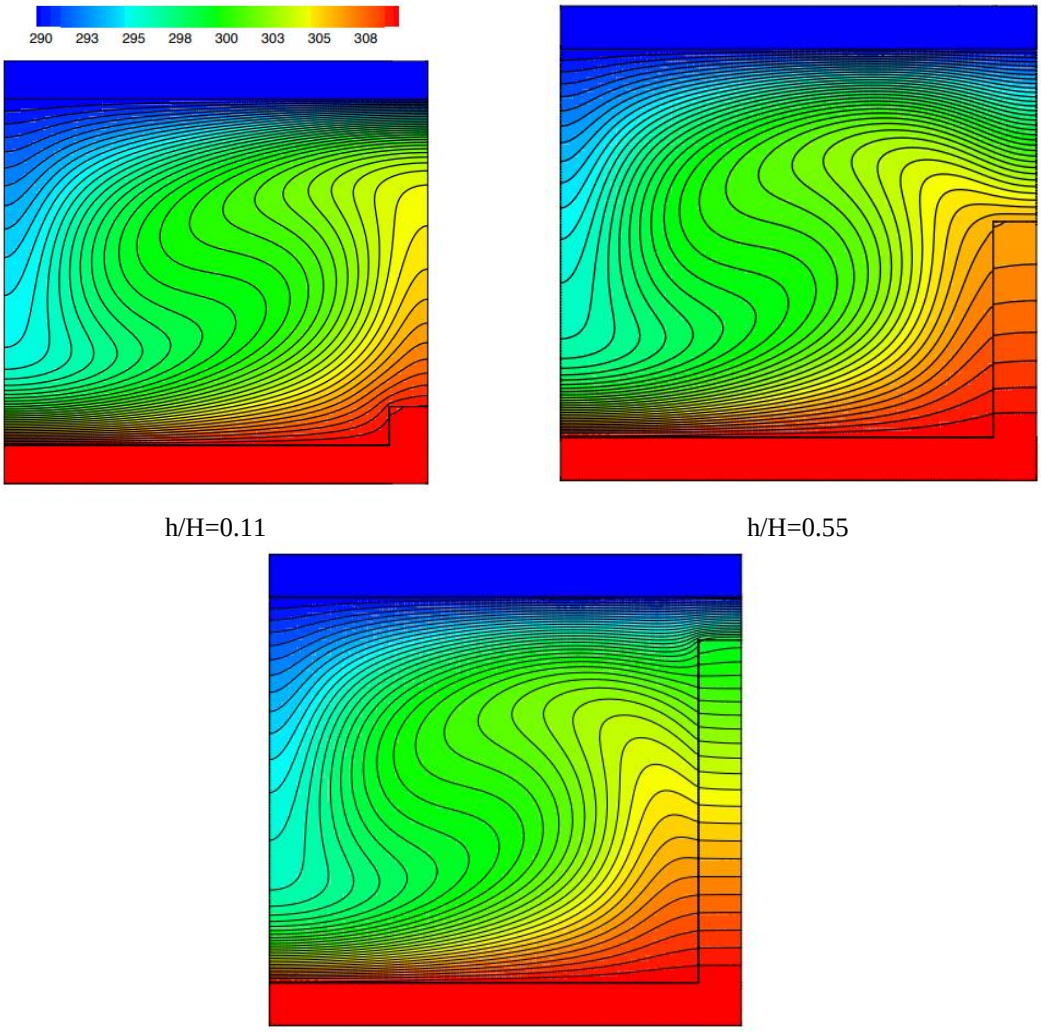

Fig. 3 Illustrative plots of the temperature field for copper fins of varying heights for fixed fin spacing of W/H=1.2 and a Rayleigh number of 1.97×10^4. The maximum temperature (red) is 310K and the minimum temperature (blue) is 290K

spacing is increased, all conduction profiles in Fig. 2 asymptote to unity as *W/H*>>1; indeed, even for *W/H* ~1 the impact of the fin is largely diminished.

3.1 Role of fin height and material

We begin by examining the impact of the fin height and thermal conductivity as a function of Rayleigh number for a fixed fin spacing. To this end, we choose the case of W/H=1.2 as a representative scenario. Illustrated in Fig. 3 are the steady-state temperature distributions for thermally-conducting (copper) fins of heights *h/H*=0.11, 0.55 and 0.88 at a Rayleigh number of

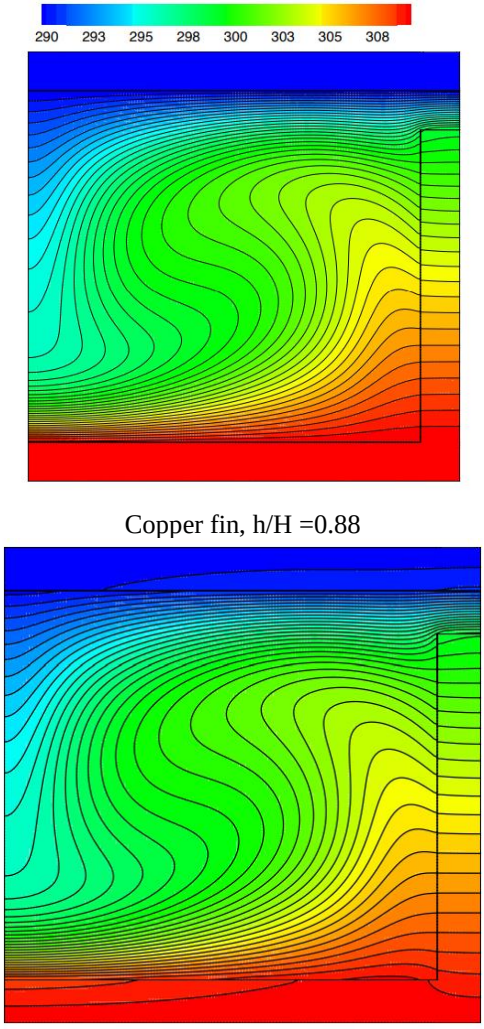

Fig. 4 Comparative plots of the temperature field for copper fins (left) and wood fins (right) for a fixed fin spacing of W/H=1.2 and fin height h/H=0.88 at a Rayleigh number of 1.97×10^4. The maximum temperature (red) is 310K and the minimum temperature (blue) is 290K

1.97×10^4. The fin height has an observable effect on the temperature field in the immediate vicinity of the fin surface; however, the temperature distribution in the remainder of the convection cell appears rather insensitive to the fin height. As the fin height increases, there is the effect of 'lateral' heating of the fluid from the fin surface. There is the interesting result that the greatest heating of the fin region appears to occur for the intermediate fin height of *h/H*=0.55. While it is intuitive that a longer fin would produce greater heating over a shorter fin as it extends further into the cell, evidently an additional mechanism is involved as the heating actually diminishes for the case of the longest fin (*h/H*=0.88). The explanation for this lies in the hydrodynamic role of the fin as a no-slip solid boundary for the weak natural convection flow. Evidently a trade-off must exist

between the additional heating provided by the extended surface and the drag effects incurred. Quantitative illustrations of this interplay are provided in subsequent sections of this article.

Figure 4 demonstrates the impact of the thermal conductivity of the fin for the parametric conditions of Fig. 3 for cases of a conducting and insulating fin. The temperature field between the two cases are very similar indicating that the choice of fin material is of minor consequence. This is consistent with the conduction results previously shown in Fig. 2. Simulations for cases of close fin spacing, not presented here, do show a slightly more noticeable difference; however, the natural convective flow in those cases is very weak and thus any differences are largely inconsequential. These observations further support the notion that the hydrodynamic role of the fin is of greater importance that its thermal property.

Given the minor importance of the thermal material, for the remainder of this article we present results only for the case of conducting (copper) fins with the implicit understanding that corresponding results for non-conducting (wood) fins will be similar in nature.

3.2 Effect of fin spacing at low Rayleigh numbers

We next quantitatively examine the heat transfer characteristics associated with different fin spacing and heights. In particular, fin spacing is varied over the range W/H=0.12-1.2 with fin heights are also variable from h/H=0.11 to 0.88. The intent is to focus on the effect of fins with spacing that imposes smaller convection cells than the Rayleigh-Bénard cells that naturally occur between infinite parallel plates. From the classic Rayleigh-Bénard stability analysis, the expected diameter D of the convection cells/rolls is equal to one-half of the critical wavelength λ_c of the most unstable mode, which is known is to be (Manneville 2006).

$$D \simeq \lambda_c \simeq 1.007\, H \tag{10}$$

Thus, the naturally occurring diameter of the convection cell is nearly equal to the height of the cell or $W/H \approx 1$. In this work, significantly larger fin spacing has also been examined to verify the trend towards the classic Rayleigh-Bénard problem, but those results are not presented here.

For the present, it is convenient to restrict the range of Rayleigh to modest levels ($Ra < 2 \times 10^4$ where the buoyant convection is relatively weak. The Nusselt numbers, as determined from the numerical simulations, appear in Figs. 5-7 where each figure corresponds to a fixed fin height of h/H=0.11, 0.55 and 0.88, respectively. For the Rayleigh numbers Ra = 1.970, 9860 and 19710 considered in each of the figure, the corresponding Nusselt numbers obtained from Eq. (8) for idealized Rayleigh-Bénard flow are Nu= 1.19, 2.38 and 2.82

Several observations can be made regarding the interaction between the effects of fin spacing, height and the Rayleigh number. First, at the lowest Rayleigh number in these cases (Ra=1971) there is no onset of convection at all for the range of fin spacing and heights considered - the system remains in a state of conduction. This Rayleigh number is only slightly larger than the critical value of Ra=1708 derived for the idealized Rayleigh-Bénard problem. Therefore, the presence of the fin introduces an inhibiting effect for the transition to a convective state at very low Rayleigh numbers. At a higher Rayleigh number of Ra=9860 one sees that the case of an intermediate fin height h/H=.55 still remains in a conduction state until a threshold fin spacing is reached (W/H ~ 0.35). A similar behaviour is observed with the tallest fin h/H=0.88 except that the threshold spacing is increased to W/H~0.45. A similar trend occurs for the largest Rayleigh number of Ra=19710 except that the threshold spacing is smaller still. As alluded to in the previous section, the existence of a fin represents, hydrodynamically, an additional solid boundary and a

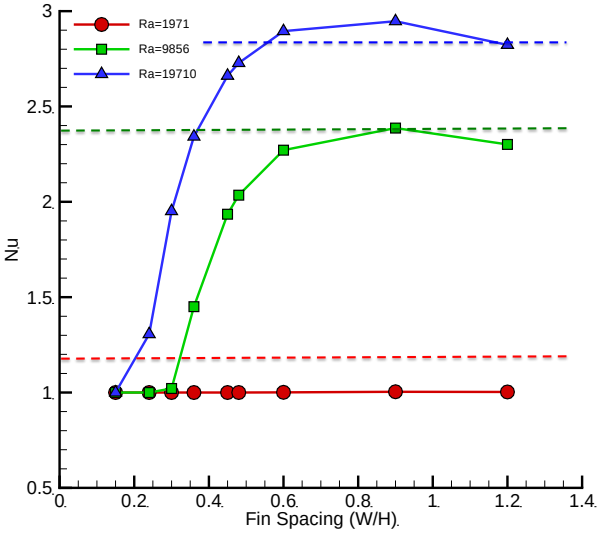

Fig. 5 Plot of Nusselt number as a function of the fin spacing (W/H) for three Rayleigh numbe rs ($Ra = 1.97 \times 10^3, 9.86 \times 10^3,$ and 1.97×10^4) and a fin height of h/H=0.11. For comparison purposes, the Nusselt numbers associated with pure Rayleigh-Bénard flow are Nu= 1.19, 2.38 and 2.82 at the respective Rayleigh numbers and are indicated by dashed lines

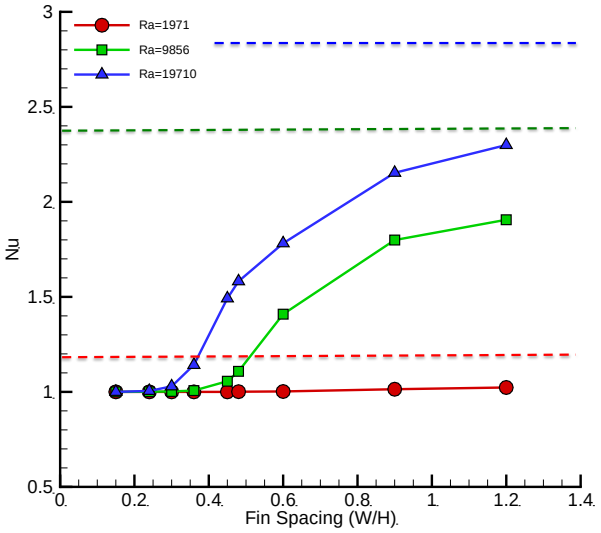

Fig. 6 Plot of Nusselt number as a function of the fin spacing (W/H) for three Rayleigh numbers $Ra = 1.97 \times 10^3, 9.86 \times 10^3,$ and 1.97×10^4) (and a fin height of h/H=0.55. For comparison purposes, the Nusselt numbers associated with pure Rayleigh-Bénard flow are Nu= 1.19, 2.38 and 2.82 at the respective Rayleigh numbers

source of friction to the buoyant flow. At the modest Rayleigh numbers being examined here, the buoyant flow is very weak and evidently the drag resulting from the fins is sufficient to stifle flow development altogether if the fins are too closely spaced. The threshold fin spacing necessary for convection onset diminishes with increasing Rayleigh number since the associated buoyancy force is increased and more able to overcome the wall drag.

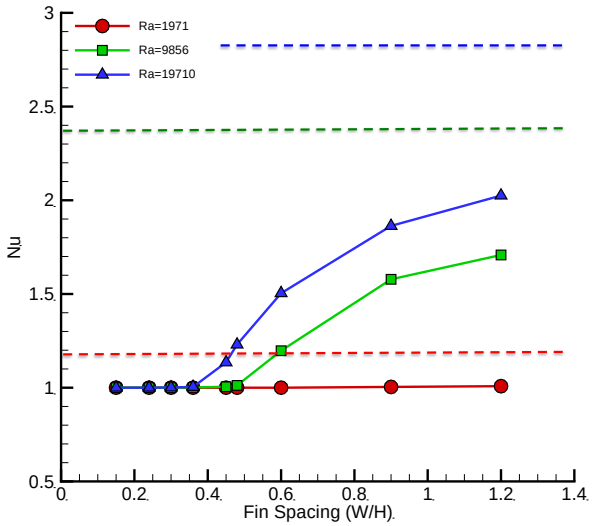

Fig. 7 Plot of Nusselt number as a function of the fin spacing (W/H) for three Rayleigh numbers ($Ra = 1.97 \times 10^3, 9.86 \times 10^3, and\ 1.97 \times 10^4$) and a fin height of h/H=0.88. For comparison purposes, the Nusselt numbers associated with pure Rayleigh-Bénard flow are Nu= 1.19, 2.38 and 2.82 at the respective Rayleigh numbers

In addition to inhibiting the onset of convection, the presence of the fin is generally seen to be detrimental to the heat transfer characteristics of the cell at low Rayleigh numbers. For the cases shown in Figs. 5-7 nearly all Nusselt numbers are below the corresponding values for the Rayleigh-Bénard cell without fins. The only exception to this trend is found in the case of a short fin (h/H=0.11) in a region of fin spacing of approximately W/H~ 0.6-1.2 where the Nusselt number matches or slightly exceeds the Rayleigh-Bénard value. A weak, local maximum occurs at $W/H \approx 0.9$. The temperature field and streamline pattern corresponding to this condition is depicted in Fig. 8a. For comparison, the temperature field and streamline pattern for the case of W/H=1.2 is shown in Fig. 8b. There are no dramatic differences seen which suggests that the optimization of the configuration is somewhat subtle in its nature. One potentially important observation can be made, however, with regards to the temperature field in the vicinity of the bottom plate for this 'optimal' configuration. It appears that the impact of the fin is to effectively replace the flat, isothermal bottom plate with a curved isothermal plate which is 'contoured' to the convection cell. This finding is suggestive of the classic, convex-parabolic optimal fin of Schmidt (1926) and also the minimum-volume fin design reported by Hanin and Campo (2003).
It is natural to contrast this 'optimal' spacing with the known cell size found in the classic Rayleigh-Bénard stability analysis. As given by Eq. (10) the idealized Rayleigh-Bénard cell size corresponds to W/H ~1; thus, the optimal spacing of W/H ~ 0.9 corresponds to a convection cell which is approximately 90\% of the Rayleigh-Bénard cell. This close similarity further underscores the subtlety of the enhancement at this low value of Ra.

3.3 Higher Rayleigh number flow for smaller fin spacings

Based upon the results of the preceding section, it is evident that fins can have a pronounced effect on the flow field and heat transfer for moderately close fin spacings. The fact that conditions

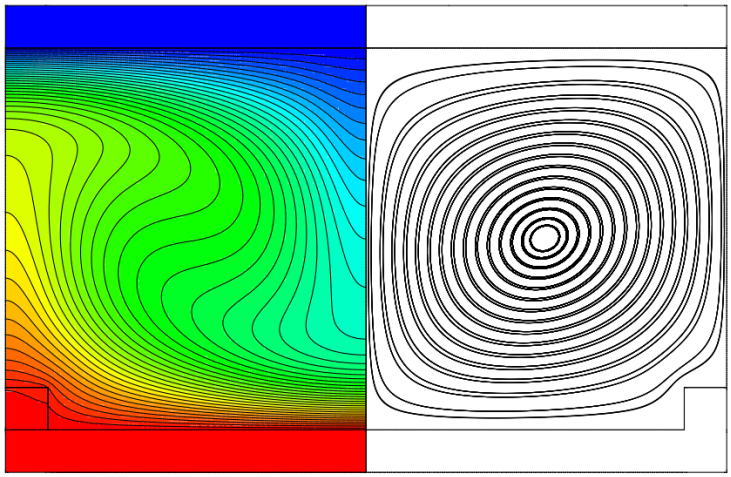

(a) Optimal spacing, W/H =0.9

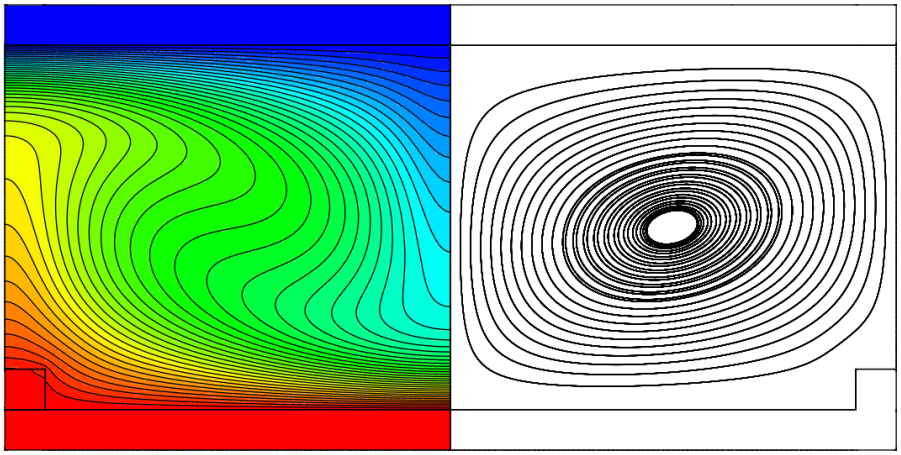

(b) W/H =1.2

Fig. 8 Comparative plots of the temperature field and streamline patterns for the (a) optimal fin spacing and (b) near-optimal fin spacing cases for small fins (*h/H*=0.11) at a Rayleigh number of 1.97×10^4.

were found to exist wherein heat transfer was enhanced over Rayleigh-Bénard theory for *W/H*<1 suggests the possibility of further enhancement at larger Rayleigh numbers and for appropriate fin configurations. Accordingly, we next examine the flow and heat transfer characteristics at higher Rayleigh numbers and restrict the focus to closer fin spacings with $W/H < 0.6$. Calculated Nussselt numbers are presented in Figs. 9-11 for a range of laminar Rayleigh numbers $Ra \sim 10^3$-10^5 for a set of fin spacings and heights. For comparison purposes, the corresponding empirical predictions for Rayleigh-Bénard flow based on Eq. (8) is included in each figure.

There are several observations to be made from this set of figures. First and foremost, one finds that the impact of the fin is *detrimental* in all configurations involving intermediate (*h/H*=0.55) and tall fin heights (h/H=0.88). In all such cases, the resulting heat transfer is less than the value that would be obtained with no fins at all; this negative impact is most pronounced for the tallest

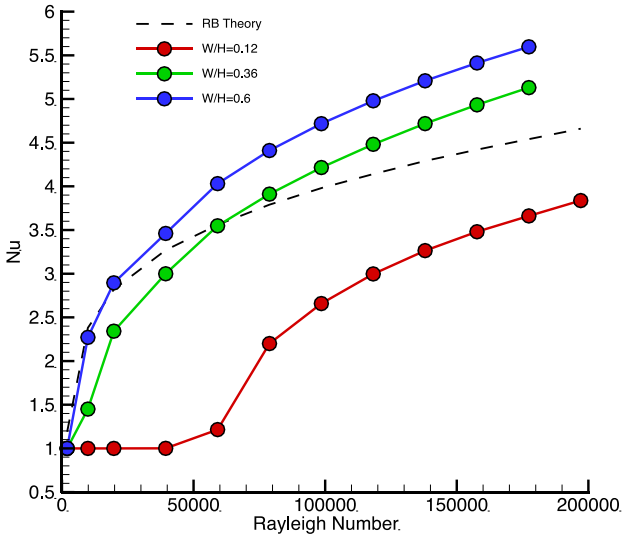

Fig. 9 Plot of Nusselt number as a function of the Rayleigh number for three different fin spacin gs (W/H=0.125, 0.33 and 0.5) and a short fin (h/H=0.11)

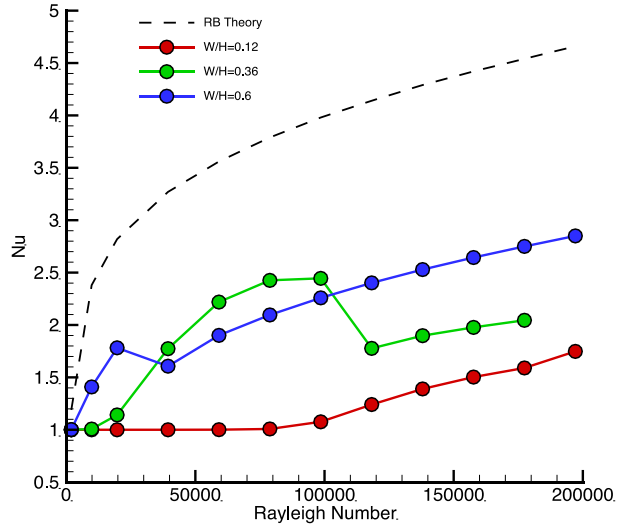

Fig. 10 Plot of Nusselt number as a function of the Rayleigh number for three different fin spacings (W/H=0.125, 0.33 and 0.5) and an intermediate fin (h/H=0.55)

fins. In contrast, for the shortest fins examined (h/H=0.11) it is seen that the heat transfer is increased except for the narrowest of fin spacings and/or at very low Rayleigh numbers. The degree of enhancement grows as the Rayleigh number is increased, but is also dependent on the fin spacing - the greatest enhancement in these cases is found for *W/H* =0.6. Taken together, these observations suggest that some optimal spacing of short fins that maximizes heat transfer is possible for flows at higher Rayleigh numbers.

For cases of intermediate and tall fins (Figs. 10-11), there is other noteworthy behaviour aside from poor heat transfer characteristics. Consistent with the results of Figs. 5-7, one again finds a

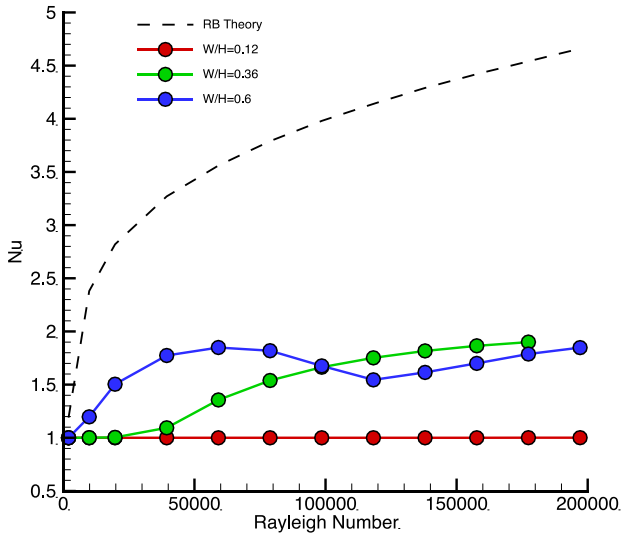

Fig. 11 Plot of Nusselt number as a function of the Rayleigh number for three different fin spacings (W/H=0.125, 0.33 and 0.5) and a tall fin (h/H=0.88)

delayed onset to convection that occurs at a threshold value of the Rayleigh number, the value of which is greatest for the tallest fins and closest fin spacings. Indeed, for the case of the tallest fin and the closest fin spacing (*W/H*=0.12) a state of pure conduction persists over the entire range of Rayleigh numbers examined. Following the onset of convection, Nusselt number curves begin to follow a power law behaviour as would be expected. For the intermediate fin height, however, the Nusselt number plots reveal additional and unexpected behaviour. Referring to Fig. 10, at fin spacings *W/H*=0.36 and 0.6 there is initial growth in *Nu* with *Ra* followed by a relatively sharp decrease at a critical value of *Ra*. Beyond this critical Rayleigh number there is again monotonic growth in *Nu*. This transition occurs earliest for the wider fin spacing and is delayed with decreasing fin spacing. A similar, though less pronounced, transition is also observed in Fig. 11 for the tall fin at the widest fin spacing. The hydrodynamic origin of this transitional behaviour is discussed next.

3.4 Flow bifurcation at critical Rayleigh numbers

As demonstrated in Figs. 10-11, under certain parametric conditions the Nusselt number was found to locally decrease with increasing Rayleigh number. Detailed examination of the velocity fields in such instances reveals that the phenomena is linked to the onset of flow separation top edge of the fin for a critical value of the Rayleigh number. The sequence of events is well depicted in Fig. 12 for an intermediate fin height (*h/H*=0.55) over a limited range of Rayleigh numbers spanning $Ra = 3.94 \times 10^4$ to 9.86×10^4. Referring to this figure, one sees that the convection pattern initially consists of a single cell. As the Rayleigh number is gradually increased flow separation occurs at the fin edge giving rise to a second counter-rotating cell which exists in the region between the fin top and the upper plate. As the Rayleigh number continues to increase this secondary cell increases in strength and moves into a position almost directly above the primary cell. Finally, at still higher Rayleigh numbers the cell pattern stabilizes in position and continues to increase in circulation. It is the flow bifurcation that occurs at the fin edge – and the transitional

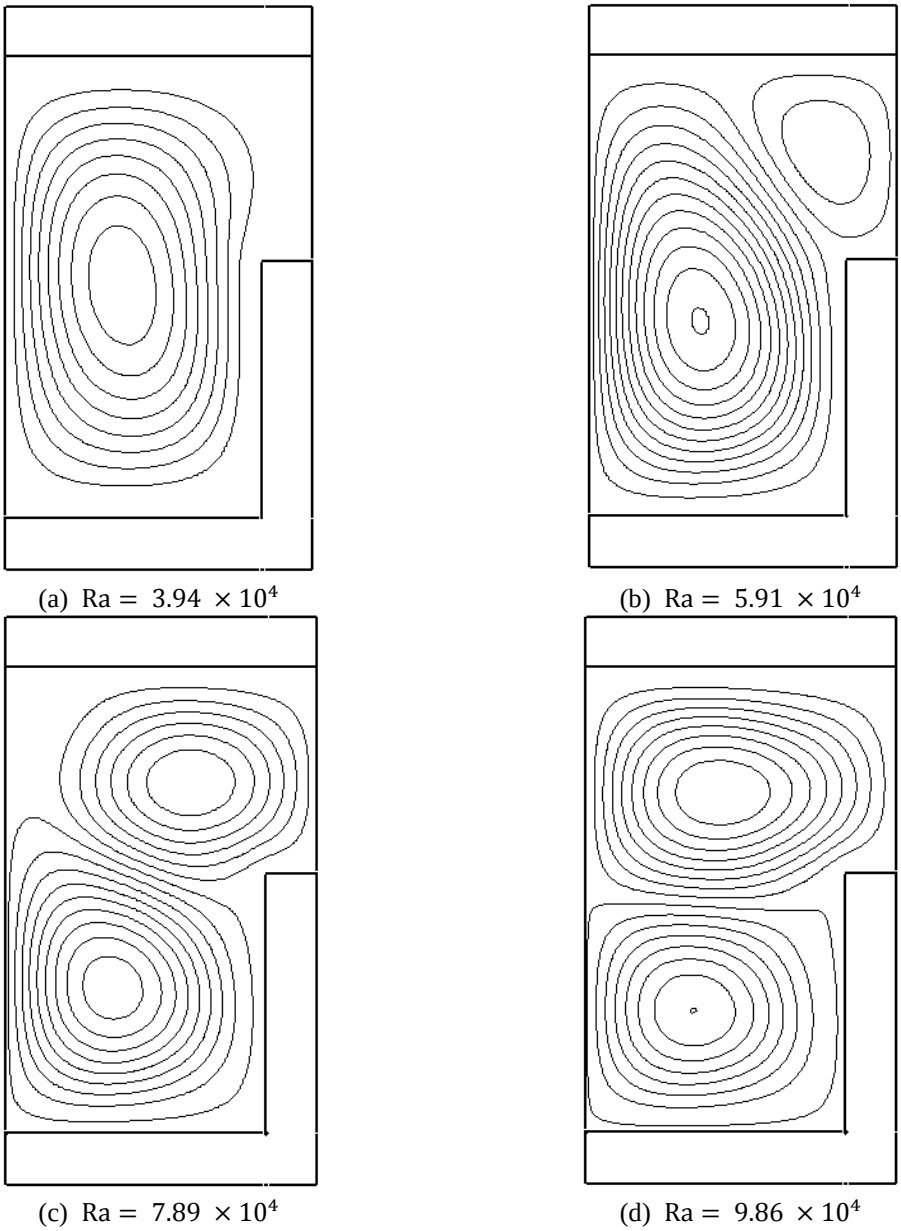

(a) $\mathrm{Ra} = 3.94 \times 10^4$ (b) $\mathrm{Ra} = 5.91 \times 10^4$

(c) $\mathrm{Ra} = 7.89 \times 10^4$ (d) $\mathrm{Ra} = 9.86 \times 10^4$

Fig. 12 Streamline plots for a copper fin geometry of W/H=0.6 and h/H=0.55 depicting the onset of a flow bifurcation at increasing Rayleigh numbers

regime for the secondary cell development – that are reflected in the local reductions in the Nusselt number plots. Once the dual cell arrangement has stabilized in its position, the increasing intensity of the cell circulation results in a subsequent monotonic increase in the Nusselt for further increases in the Rayleigh number. The net effect of this dual cell configuration, however, is a heat transfer performance that is well below that of the Rayleigh-Bénard scenario.

The height of the fin is found to impact the development of the secondary convection cell, as

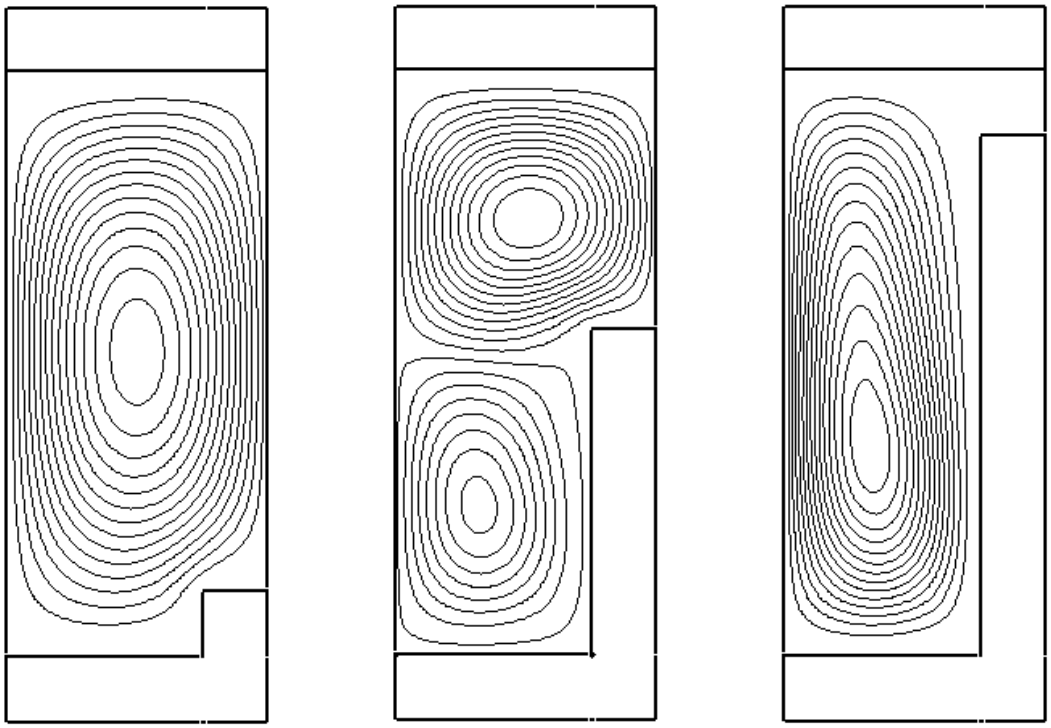

h/H = 0.11 h/H = 0.55 h/H = 0.88

Fig. 13 Plots streamline patterns for three different fin heights at a fin spacing of W/H=0.36 and Ra = 1.18×10^5. The fin configuration is such that a single roll pattern exists for the smallest and tallest fins; however, for h/H=0.55 a flow separation at the upper edge of the fin gives rise to a dual convection cell arrangement

depicted in Fig. 13. For the shortest of fins, the fluid velocity at the top of the fin is evidently insufficient for flow separation to occur due to the close proximity to the bottom of the cavity. Consequently, the Nusselt plots do not exhibit any bifurcation phenomena. A similar situation occurs for the tallest of fins. Here the close proximity to the upper plate decelerates the flow and thus inhibits separation; instead a single cell remains whose center is skewed towards the bottom of the enclosure. Only for the intermediate fin height is the flow state commensurate with the conditions necessary for separation to occur.

Yet another fin parameter that plays a role in the occurrence of flow separation is the fin thickness *t/H*. Specifically, it is expected that a fin of sufficient thickness is required to generate the necessary adverse pressure gradient to cause the separation. As such, it is expected that for a sufficiently thin fin the separation should cease. This consideration has been investigated by examining cases of two reduced fin thicknesses *t/H*=0.055 and 0.011 in Fig. 14. These cases correspond to fin thicknesses of 50% and 10%, respectively, of the default fin thickness used throughout this study. It is found that elimination of the flow separation is indeed possible provided an extremely thin fin (*t/H*=0.011) is used. In practical terms, the imposition of a design constraint on the fin thickness in an experimental system would be unlikely to present a significant technical challenge; nonetheless, this aspect cannot be ignored if the possibility of flow separation is to be avoided.

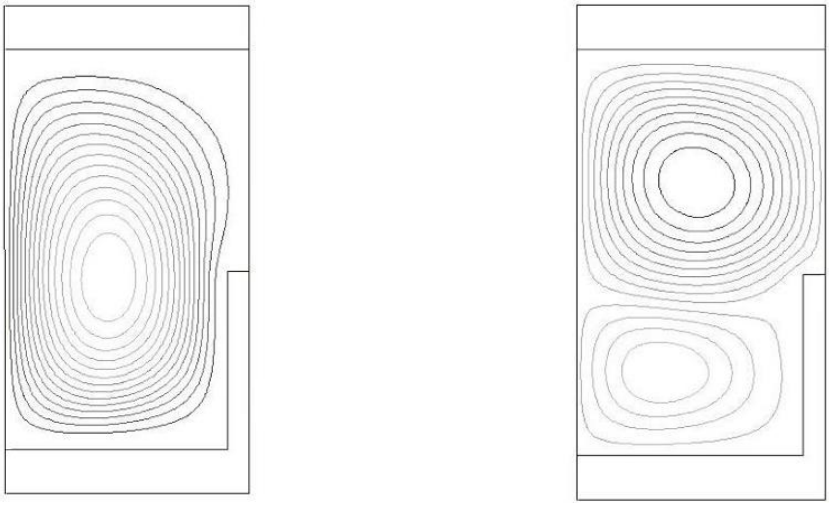

(a) $\mathrm{Ra} = 1.18 \times 10^5$ (b) $\mathrm{Ra} = 1.58 \times 10^5$

(c) $\mathrm{Ra} = 1.18 \times 10^5$ (d) $\mathrm{Ra} = 1.58 \times 10^5$

Fig. 14 Streamline plots for thin, conducting fins of thicknesses t/H=0.055 (top) and t/H=0.011 (bottom) at two different Rayleigh numbers for W/H=0.6 and h/H=0.55. Elimination of flow bifurcation is possible for a sufficiently thin fin

4. Discussion

At this stage, it is worthwhile to summarize the numerical heat transfer results obtained for the various fin configurations and to frame this within the context of Rayleigh-Bénard theory. For all but the shortest of fins, the heat transfer obtained for with fin spacings $W/H<1$ was found to be less than that for the Rayleigh-Bénard scenario without fins. However, for very short fins, one does see that a noticeable enhancement of heat transfer is possible for the range of conditions examined. The use of very short fins and fin spacings less that $W/H< 1$ has the effect of imposing a smaller convection cell size than would naturally occur in the Rayleigh-Bénard stability analysis. The circulation patterns for the smaller cells are evidently increased over that present in the Rayleigh-

Bénard cell and hence leads to large convective transfer. However, the precise nature of the enhancement remains somewhat unclear. Examination of the temperature field and the velocity fields for the enhanced heat transfer cases suggests that a possible explanation may lie in an analogy to the classic, optimal fin of Schmidt (1926) in that the presence of the fin produces an effectively 'curved' lower boundary which is approximately convex-parabolic.

A key finding in this study is that the impact of the fin is almost entirely due to its hydrodynamic role as a no-slip boundary condition. The thermal impact of the fin, as an extension of the bottom plate of the enclosure into the gap, is insignificant and thus renders the selection of fin material moot. Taken together, the combined effect of fin spacing and height can be regarded as a retarding force whose origin lies in frictional forces at the solid boundaries. For cases of tall, closely-spaced fins the buoyant forces are substantially comprised which reduces the convection intensity and consequently the heat transfer capacity-indeed, for sufficiently 'confined' geometries and low Rayleigh number the solid boundaries can inhibit convection altogether. For sufficiently thick and tall fins with adequate spacings and at moderate laminar Rayleigh numbers, heat transfer performance can also be compromised due to unwanted flow separation and the formation of a secondary convection cell.

It is reasonable to expect that the retarding hydrodynamic effects of taller fins should become less pronounced as flow inertia increases at still higher Rayleigh numbers, including the turbulent flow regime. These higher Rayleigh number conditions are beyond the scope of the present study and have not been examined here. Despite the expectation of improved performance at higher Rayleigh numbers, there appears to be little justification for the selection of taller fins over short fins based on the findings of this work.

In terms of comparisons with related findings in the heat transfer literature, the experimental study by Inada *et al*. (1999) is the most relevant. In their work, three different fin spacings (W/H=0.525, 0.7 and 1.05) were explored with a fixed, moderate fin height h/H=0.5. Both conducting and non-conducting fin materials were used and the fin thickness was fixed at t/H=0.05. Measurements of the local and average Nusselt number were made at six values of the Rayleigh number between 5,000-20,000 (approximately). Heat transfer measurements with fins were contrasted with those obtained for a simple Rayleigh-Bénard cavity without fins and having a finite 8:1 aspect ratio. Based on these experimental conditions, a significant overlap thus exists with the parametric conditions of this computational study and a comparison of the findings is warranted. Their experiments showed that a fin spacing of W/H=1.05 slightly outperformed the case of W/H=0.7$, which in turn outperformed the case of W/H=0.525; in other words, decreasing the fin spacing among these cases diminished the heat transport. The smallest spacing of W/H=0.525 performed noticeably worse, including the observation of a pure condition state for a non-conducting fin material (balsa). For conducting fins, only the case of W/H=1.05 yielded an enhancement of heat transfer over the experimental Rayleigh-Bénard cavity. The case of W/H=0.7 yielded roughly the same degree of heat transport as the Rayleigh-Bénard cavity and the closest fin spacing of W/H=0.525 resulted in a decrease in heat transport.

Overall, the experimental findings of Inada *et al*. (1999) compare favourably with those obtained in this computational study for common parametric conditions. The experiments, in particular, confirm that the introduction of fins into a Rayleigh-Bénard cavity at laminar Rayleigh numbers can lead to a modest increase in heat transport (~20%) under a favourable fin configuration; however, in many cases the impact of the fins is detrimental. The experimental work also confirms that the thermal conductivity of the fin material has a largely insignificant effect on the heat transfer augmentation.

5. Conclusions

In this work, a comprehensive numerical investigation has been performed to delineate the impact of transverse fins on heat transport within Rayleigh-Bénard enclosures. The focus has been on low Rayleigh number flows corresponding to likely aerospace avionics passive cooling scenarios. The relative impacts of various fin configuration parameters – fin spacing, height, thickness and thermal conductivity – have been delineated over a range of laminar Rayleigh numbers. As such, this work represents an important extension to the previous experimental studies of Inada *et al*. (1999). The computational results have revealed that surprisingly rich fluid mechanical behavior is possible under certain parametric conditions, including flow bifurcations leading to dual-convection cells not found in the traditional Rayleigh-Bénard problem.

The net heat transfer augmentation is found to result from a combination of competing fin effects, most of which are hydrodynamic in nature. Thermal aspects of the fin appear to contribute little to the observed behavior. Heat transfer enhancement is possible under certain operating conditions and for appropriate fin configurations. Favorable fin configurations are generally characterized by short, thin fins with spacings in the approximate range of W/H =0.5-1.0 and the fin performance improves with larger Rayleigh numbers. The importance of utilizing a short, thin fin is the definitive outcome of this study. The hydrodynamic impact of the n is such that its sole useful purpose is to impose a convection cell diameter and shape within the Rayleigh-Bénard cavity that enhances the heat transfer. Excess fin height only serves to retard ow circulation because of the no-slip surface, sufficiently thick fins can result in unwanted ow separation and bifurcation.

The maximum level of enhancement found for the operating conditions of this study was approximately 1.2 times greater than the corresponding expectation from Rayleigh-Bénard theory. In contrast, for unfavorable configurations the ns were found to be detrimental and the heat transport was less than for a Rayleigh-Bénard enclosure with no fins at all. The numerical data suggests that, in principle, an optimal fin configuration should exist for a given Rayleigh number that maximizes heat transfer. That said, the data also suggests that the heat transfer maximum associated with the optimal fin configuration may not be especially pronounced.

Acknowledgments

Portions of this work was supported by the National Aeronautics and Space Administration under NASA Cooperative Agreement NCC5-581 (DLH). The authors would like to acknowledge Professor A. Campo for identifying the potential for a numerical study based on the experiments of Inada *et al*. (1999).

References

Ahmadi, M., Mostafavi, G. and Bahrami, M. (2014), "Natural convection from rectangular interrupted fins", *J. Therm. Sci*., **82,** 62-71.

Amraqui, S., Mezrhab, A. and Abid, C. (2011), "Combined natural convection and surface radiation in solar collector equipped with partitions", *Appl. Solar Energy*, **47**(1), 36-47.

Arquis, E. and Rady, M. (2005), "Study of natural convection heat transfer in a finned horizontal fluid layer", *J. Therm. Sci*., **44**(1), 43-52.

Beldar, K. and Patil, A. (2017), "Fabrication and CFD analysis of cylindrical heat sink having longitudinal fins with rectangular notches", *Res. J. Eng. Technol.*, **4**(6), 678-684.
Bergles, A.E. (1999), "Techniques to enhance heat transfer", *Handbook of Heat Transfer*, McGraw-Hill, New York, U.S.A.
Catton, I. (1978), "Natural convection in enclosures", *Proceedings of the 6th International Heat Transfer Conference*, Toronto, Canada, August.
Hanin, L. and Campo, A. (2003), "A new minimum volume straight cooling fin taking into account the length of arc", *J. Heat Mass Transfer*, **46**(26), 5145-5152.
Hollands, K.G.T., Unny, T.E., Raithby, G.D. and Konicek, L. (1976), "Free convective heat transfer across inclined air layers", *J. Heat Transfer*, **98**(2), 189-193.
Hoogendoorn, C.J. (1986), "Natural convection in enclosures", *Proceedings of the 8th International Heat Transfer Conference*, San Francisco, U.S.A., August.
Inada, S., Taguchi, T. and Yang, W.J. (1999), "Effects of vertical fins on local heat transfer performance in a horizontal fluid layer", *J. Heat Mass Transfer*, **42**(15), 2897-2903.
Jaluria, Y. (2003), "Natural convection", *Heat Transfer Handbook*, John Wiley and Sons, New Jersey, U.S.A.
Kanashima, Y., Nishino, K. and Yoda, S. (2005), "Effect of g-jitter on the thermocapillary convection experiment in the ISS", *Microgravity Sci. Technol.*, **16**(1), 285-289.
Lin, N.N. and Bejan, A. (1983), "Natural convection in a partially divided enclosure", *J. Heat Mass Transfer*, **26**(12), 1867-1878.
Manglik, R.M. (2003), "Heat transfer enhancement", *Heat Transfer Handbook*, John Wiley and Sons, New Jersey, U.S.A.
Manneville, P. (2006), "Rayleigh-Benard convection: Thirty years of experimental, theoretical and modeling work", *Dynamics of Spatio-Temporal Cellular Structures*, Springer, New York, U.S.A.
Naumann, R.J. (2000), "An analytical model for transport from quasi-steady and periodic accelerations on spacecraft", *J. Heat Mass Transfer*, **43**(16), 2917-2930.
Nelson, E.S. (1994), "An examination of anticipated g-jitter on space station and its effects on materials processes", NASA-TM-103775, E-6042, NAS 1.15:103775; NASA Lewis Research Center, Cleveland, U.S.A.
Ostrach, S. (1972), "Natural convection in enclosures", *Adv. Heat Transfer*, **8**(1), 161-227.
Papari, M.M., Hitt, D.L. and Campo, A. (2005), "Dual influence of temperature and gas composition of selected helium-based binary gas mixtures on the thermal convection enhancement in Rayleigh-Bénard enclosures", *J. Heat Mass Transfer*, **48**(23), 5081-5088.
Qarnia, H.E., Draoui, A. and Lakhal, E.K. (2013), "Computation of melting with natural convection inside a rectangular enclosure heated by discrete protruding heat sources", *Appl. Math. Model.*, **37**(6), 3968-3981.
Rayman, M.D., Fraschetti, T.C., Raymond, C.A. and Russell, C.T. (2006), "Dawn: A mission in development for exploration of main belt asteroids Vesta and Ceres", *Acta Astronautica*, **58**(11), 605-616.
Schmidt, E. (1926), *Die Wärmeübertragung durch Rippen*, Germany.
Singh, K.K. and Sinha, M.K. (2016), "Parametric effects on a heat sink with branched fins under natural convection", *J. Sci. Eng. Res.*, **7**(6), 229-236.
Sivaprakasam, V. Basha, J.K., Udhayarasu, R. and Siva, D. (2015), "Experimental investigation on the performance of longitudinal fins with different notches using mixed convection heat transfer", *J. Res. Aeronaut. Mech. Eng.*, **3**(6), 12-20.

EC